Journal of the European Ceramic Society 19 (1999) 1759–1767

PII: S0955-2219(98)00275-1
0955-2219/99/$ - see front matter

Experimental and Numerical Study of Grain Growth in Alumina Fibres Heat Treated at 1700°C

J. M. Heintz,* J. C. Bihr and J. F. Silvain

ICMCB-CNRS, Université Bordeaux I, Av. Dr Schweitzer, F-33608 Pessac Cedex, France

(Received 12 October 1998; revised version received 2 November 1998; accepted 7 November 1998)

Abstract

The studied material is an alumina fibre acting as a reinforcement in a $NiAl/Al_2O_3$ composite. The processing of this composite involves a 1700°C heat treatment. Grain growth phenomena taking place within the fibre during that step are investigated. Above 1600°C, the size of the grains reach the fibre diameter for a 1 h heat treatment. Further morphological evolution is discussed using thermodynamic calculations. Taking into account the presence of the liquid alloy, a deepened grain boundary groove is predicted and experimentally observed. The second part of this work deals with grain growth modelling during the heating and cooling steps. A cubic grain growth kinetics law is found and is used to predict final grain sizes as a function of heating and cooling rates. © *1999 Elsevier Science Limited. All rights reserved*

Keywords: modelling, grain growth, fibres, Al_2O_3, composites.

1 Introduction

The need for high temperature materials destined for aeronautic and aerospace applications has led to many studies on intermetallic materials. For example, β-NiAl phase is considered as a good candidate for uses at elevated temperatures[1] because of its high melting temperature (1640°C), its excellent resistance to oxidation combined with a low density ($5{\cdot}86\,g\,cm^{-3}$) and a high elastic constant (300 GPa). However, this intermetallic presents some disadvantages such as lack of room-temperature ductility and toughness and a low strength and creep resistance at high temperature which limit its use as a thermostructural material. Therefore, incorporation of a suitable reinforcement such as alumina fibres has been proposed to overcome these disadvantages.[2]

The composite approach implies that the fibres should be thermally stable in the used temperature range. Now, the liquid infiltration route, which was chosen to process the composite, requires a temperature of $\approx$1700°C. Although very little chemical reaction was observed between the NiAl matrix and the alumina fibre,[3] morphological evolution of the fibre must be considered. Indeed, from a thermodynamic point of view, lowering of the free energy of the dense system can be obtained by a decrease of the interfacial and grain boundary areas, which is made possible by mass transport occurring at these high temperatures. So, the aim of this work was to characterise and model morphological evolution of fibres under these severe conditions.

In the first part of this work, grain growth within alumina fibres will be presented as a function of temperature to highlight the influence of the heat treatment. Around 1700°C, the average size of the grains reached the diameter of the fibre leading to the so-called 'bamboo configuration'. Further isothermal evolution, i.e. grain boundary grooving, will be discussed based on a thermodynamic approach originally proposed by Lange and coworkers.[4] Thermodynamic calculations performed on a idealised geometry will be detailed taking into account the presence of the liquid alloy.

The second part of this work deals with a kinetic study of grain growth in order to be able to define conditions that limit grain growth and avoid undesirable grooving phenomena. Simulation of the grain growth that occurs during heating and cooling will be developed. First, the kinetic grain growth law and the corresponding activation

*To whom correspondence should be addressed. Fax: +33-556-84-8321; e-mail: heintz@icmcb.u-bordeaux.fr

energy will be determined. Second, calculations based on these values will be performed as a function of heating and cooling rates and the results compared to experimental grain sizes in order to validate our modelling. Finally, a processing schedule will be proposed from the proposed simulations.

2 Experimental

$NiAl/Al_2O_3$ composites were prepared using a liquid infiltration method.[2] In a first step, a carbon crucible containing a fibre alumina preform and the NiAl powder set above the preform were heated using a high frequency (H.F.) coil. Once the melting temperature of the NiAl matrix was reached, an argon gas pressure (30 bars) was applied to promote the flow of the liquid alloy.

Polycrystalline α alumina fibres (purity $>99{\cdot}5\%$, Almax, Mitsui Mining company) were the material under investigation. A 900°C heat treatment was performed on the yarns to remove the organic sizing agent. The fibre diameter, around $10\,\mu$m, and the initial roughness and grain size ($\sim 0{\cdot}3\,\mu$m) can be seen in Fig. 1.

Two different types of thermal treatments were applied to the alumina fibres. The first one corresponded to the study of grain size evolution versus temperature. An Al_2O_3 fibre yarn was heat treated for 1 h at different temperatures between 1300 and 1700°C. The second one was related to grain size evolution as a function of heating and cooling rates between 1400 and 1700°C. The high rates used, comprised between 3 and $35°C\,s^{-1}$, are described in more detail in Section 3.3.1. For the two procedures, experimental conditions were identical and related to the composite preparation process: carbon crucible, H.F. heating apparatus, argon atmosphere. Temperature of the carbon crucible was determined from optical pyrometer measurements (accuracy $\pm 1\%$). Average grain sizes were calculated using the linear intercept technique[5] on fractured fibres examined by scanning electron microscopy (SEM).

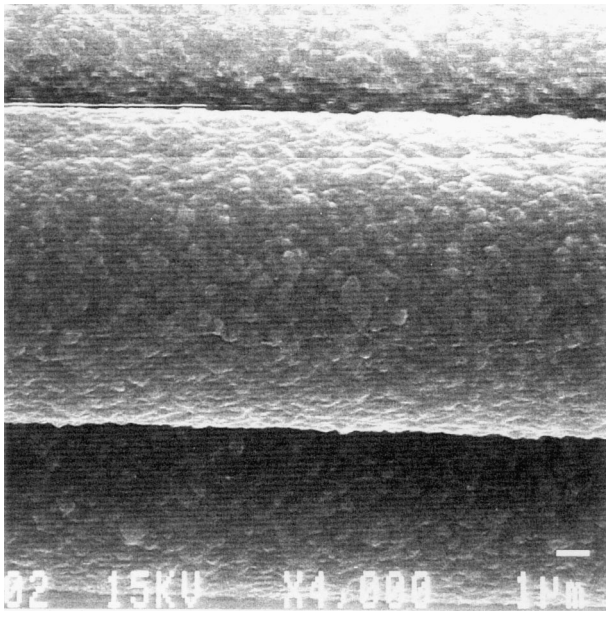

Fig. 1. SEM micrograph of alumina fibres after de-sizing treatment at 900°C.

3 Results and Discussion

3.1 Evolution of grain size as a function of the temperature

SEM micrographs of heat treated fibres are presented in Fig. 2. The size of the grains remains almost unchanged ($\approx 0{\cdot}3\,\mu$m) after a 1300°C treatment [Fig. 2(a)]. At 1400°C Fig. 2(b)], grain growth begins and this phenomenon clearly goes on at 1500°C [Fig. 2(c)]: polygonisation of the grains can be observed accompanied by a large increase of the grain size. At 1600°C [Fig. 2(d)], sections of the fibres reveal that the size of some grains reaches the diameter of the fibre. The grain growth behaviour is summarised in Fig. 3 where the average grain size is reported as a function of the temperature for a 1 h heat treatment. A sharp increase in grain size is observed above 1400°C and the average grain size reaches the fibre diameter between 1600 and 1700°C.

3.2 Evolution of fibre morphology once grain size reaches fibre diameter

When the grain size equals the fibre diameter, the grain boundaries tend to form flat surfaces normal to the axis of the fibre. In that configuration, the driving force for boundary migration tends to zero which does not favour subsequent grain growth. Nevertheless, morphological changes can still occur due to surface energy minimisation. This further evolution is then considered using Lange's thermodynamic approach.[4] It needs a simplified representation of the material to calculate and minimise its free energy.

The morphology of the fibre at that point, can be schematised by a 'bamboo'-like configuration: the fibre, of diameter d, is constituted of cylindrical grains of length L [Fig. 4(a)]. Geometrical assumptions are (i) grain centres are fixed (alumina fibres constituted a preform, rigid enough to constrain and prevent shrinkage along their axis), (ii) grains develop a barrel shape during grain boundary grooving [Fig. 4(b)]. Moreover, it is assumed that each grain retains its initial mass. The free energy of each grain is given by:

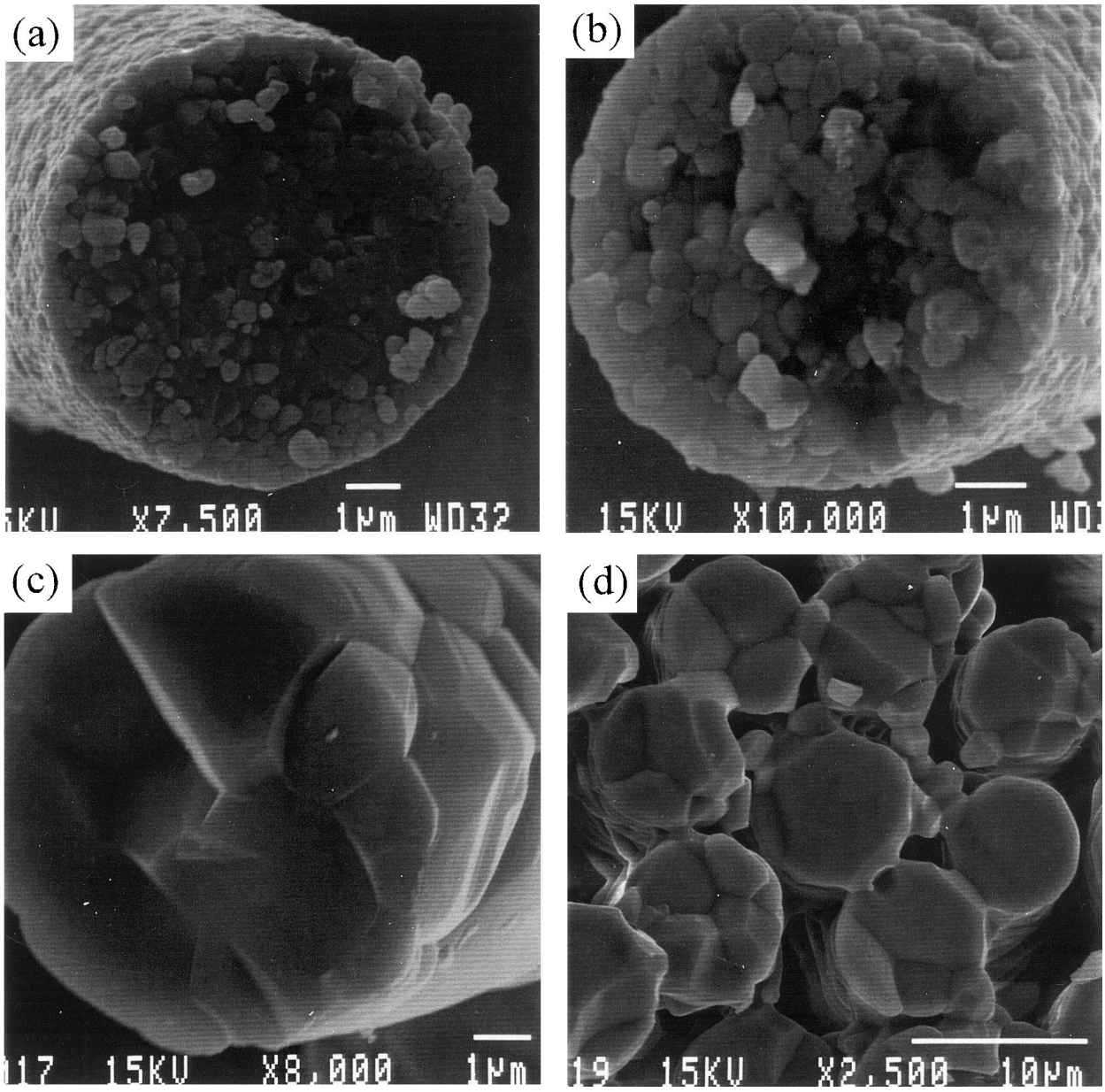

Fig. 2. SEM micrographs of sections of alumina fibres heat treated for 1 h at (a) 1300°C, (b)1400°C, (c) 1500°C, (d) 1600°C.

$$E = \gamma_s \cdot A_s + \gamma_b \cdot A_b \tag{1}$$

where A_s is the grain surface area, A_b is the grain boundary area, γ_s is the specific surface energy and γ_b is the specific grain boundary energy. The surface and grain boundary area of each grain can then be expressed as a function of d, L and ψ which describes the deepening of the grain boundary groove [Fig. 4(b)]. Calculation of the normalised free energy of the barrel shape configuration gives:

$$\frac{E}{E_o} = \frac{2a^2}{2a + \cos(\psi_e/2)}\left[\frac{1}{\sin\alpha} + \frac{\alpha}{\sin\alpha}\left(\frac{2r}{L} - \frac{\cos\alpha}{\sin\alpha}\right) + 2\left(\frac{r}{L}\right)^2 \cos(\psi_e/2)\right] \tag{2}$$

where E_o is the energy of the initial bamboo configuration, $a = L/d$, r is the radius of the grain boundary, $\alpha = (\pi - \psi)/2$ and ψ_e is the equilibrium dihedral angle derived from Young's relation.

In fact, the expression (2) is valid only for values of ψ higher than the dihedral angle corresponding to the disappearance of the grain boundary ($r = 0$). Beyond that point, separated grains can still decrease their free energy by becoming spherical [Fig. 4(c)].

Now, we propose to apply this simple approach to the studied experiment. First of all, the preparation of the $NiAl/Al_2O_3$ composite involves a liquid infiltration route. Therefore, the boundary and surface energies will be defined respectively as solid–solid (γ_{ss}) and solid-liquid (γ_{sl}) energies and related according to Young's relation:

$$2\cos\left(\frac{\psi_e}{2}\right) = \frac{\gamma_{ss}}{\gamma_{sl}} \tag{3}$$

Second, these interface energies were explicitly considered for the $NiAl/Al_2O_3$ couple at 1700°C (temperature higher than the melting temperature of NiAl and initially chosen for the processing of the composite).

The solid–solid energy was determined by Nikopoulos[6] and expressed as:

$$\gamma_{ss} = 1{\cdot}913 - 0{\cdot}611 \times 10^{-3} T(J\,m^{-2} \text{ and } T \text{ in } K),$$
$$\text{leading to : } \gamma_{ss}^{1700^\circ C} = 0{\cdot}71\ J\,m^{-2}$$

The solid–liquid energy was calculated from the usual wetting equation:

$$\gamma_{sv} = \gamma_{sl} + \gamma_{lv} \cdot \cos\theta \qquad (4)$$

Liquid–vapour and solid–vapour energies were obtained from literature data. NiAl liquid–vapour energy was estimated to be: $\gamma_{lv} = 1{\cdot}45\ J\,m^{-2}$.[7] Nikopoulos also gave the expression of solid–vapour energy in alumina[6]

$$\gamma_{sv} = 2{\cdot}559 - 0{\cdot}784 \times 10^{-3} T(J\,m^{-2} \text{ and } T \text{ in } K),$$
$$\text{leading to : } \gamma_{sv}^{1700^\circ C} = 1{\cdot}01\ J\,m^{-2}$$

The value of θ was determined at $T = 1700^\circ C$ by a Sessile drop experiment where a liquid NiAl droplet was set on a flat alumina substrate under Argon atmosphere. The contact angle was found to be equal to $\theta = 80°$.[2] The value of the solid–liquid energy deduced from eqn (4) is then: $\gamma_{sl}^{1700^\circ C} = 0{\cdot}76\ J\,m^{-2}$.

Finally, using relation eqn (3) and the above energies, the equilibrium dihedral angle is calculated: $\psi_e = 125°$.

From this value and relation eqn (2), it is possible to follow the morphological evolution of the alumina fibre immersed in liquid NiAl. For that purpose, evolution of the normalised energy of a grain (E/E_o) is plotted as a function of ψ (Fig. 5).

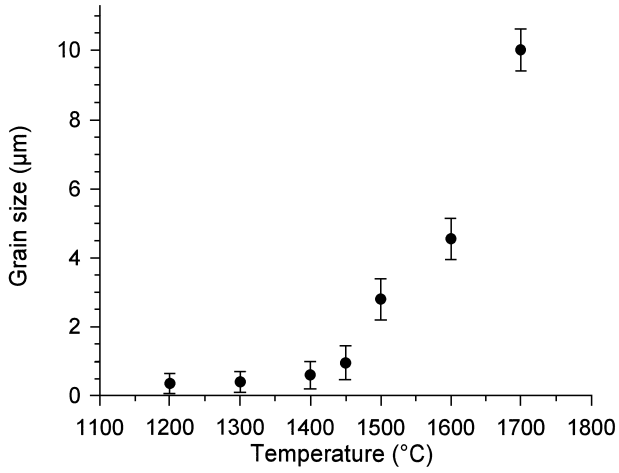

Fig. 3. Evolution of average grain size as a function of the temperature for a 1 h treatment.

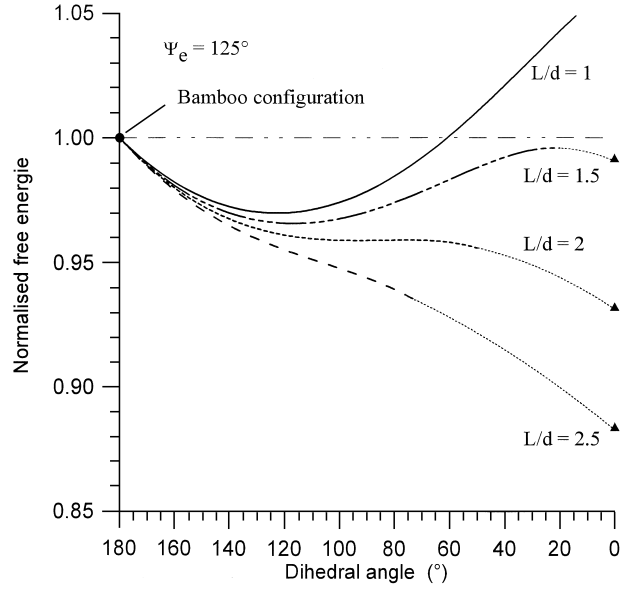

Fig. 5. Evolution of the normalised grain energy as a function of ψ and initial grain aspect ratio $a = L/d$.

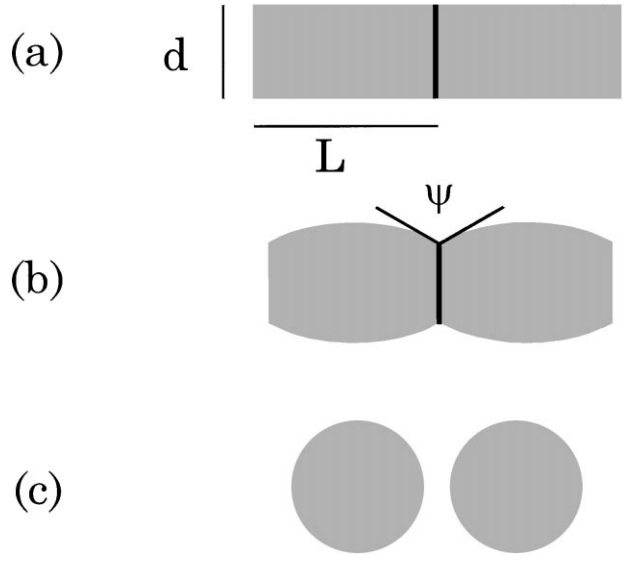

Fig. 4. Scheme of the evolution of the fibre grain morphology: (a) bamboo configuration, (b) barrel configuration, (c) spherical grains.

As the thermal treatment is proceeding at 1700°C, mass transport occurs which allows the dihedral angle, ψ, to decrease from 180° (initial bamboo like configuration) to a given value corresponding to a lower free energy. Four initial grain aspect ratio were considered in this calculation ($L/d = 1$, 1·5, 2 and 2·5).

For the first two initial configurations ($L/d = 1$ and 1·5), a minimum of free energy is observed around $\psi = 125°$ which means that grooving is expected while the fibre is still continuous.

For $L/d = 2$, a metastable energy configuration is observed around $\psi = 125°$. The final configuration ($\psi = 0$) is lower in energy but metastably attainable.

For the $L/D = 2{\cdot}5$ condition, a continuous decrease of the grain energy takes place up to the separation of the grains and can continue until grains become spherical. This case leads to a complete break up of the fibre into isolated spheres.

This calculation shows that the breaking up of the fibre needs a high initial value of the grain aspect ratio, when the size of the grains reaches the fibre diameter. This configuration is unlikely for these alumina fibres since isotropic grain growth is expected and has been actually observed.[8] An experimental confirmation was obtained from microstructure characterisation of a yarn of alumina infiltrated by the liquid NiAl matrix after composite processing at 1750°C for 15 min. After matrix dissolution, the SEM micrograph (Fig. 6) shows continuous fibres, highly grooved and preferentially made of spheroidal grains. This morphology corresponded well to the theoretical model with $L/d < 2$ and an equilibrium dihedral angle (ψ_e) close to 125°.

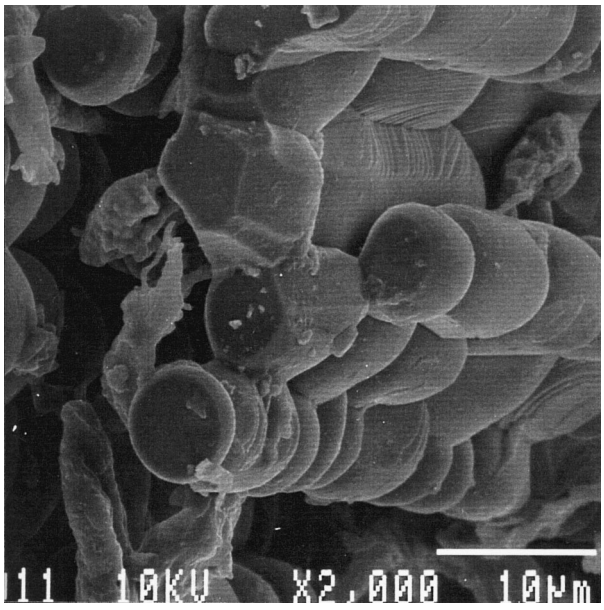

Fig. 6. SEM micrograph of alumina fibres taken from a composite prepared at 1750°C for 15 min.

3.3 Grain growth during heating and cooling of the fibres

The above results showed that the alumina fibre, heat treated at high temperature, spontaneously evolves towards a spheroidal grain string configuration which drastically lowers its mechanical properties and prevents its use as reinforcement.[9] In order to avoid that undesirable evolution, a control of the growth of the grains has to be obtained so that the initial bamboo configuration is not reached. The temperature being imposed by the processing method (melting temperature of NiAl is 1640°C), the only parameters that can be changed are heating and cooling schedules.

3.3.1 Heating and cooling kinetics

In a first step, heating and cooling rates which could be experimentally performed using our H.F. furnace equipment were determined. Evolutions of the sample temperature as a function of time are presented in Fig. 7. A short heating stage could be reached (less than 1 min) while the cooling stage was imposed by our experimental device and was almost the same whatever the previous heating treatment. These processing kinetics were mathematically fitted in order to be used in simulations. Heating and cooling experimental values were best described using exponential or power laws.

The heating stage is correctly fitted by the relation:

$$T = a \cdot t^b \qquad (T \text{ in } °C) \tag{5}$$

a and b are terms that can be related to the electrical power used. Figure 7 also reports calculated heating curves, using the values of a and b given in Table 1. The cooling stage is expressed by the relation:

$$T = c \cdot e^{-d \cdot t} \qquad (T \text{ in } °C) \tag{6}$$

c depends on the time needed to reach the maximum temperature (T_{max}) while d is a constant for

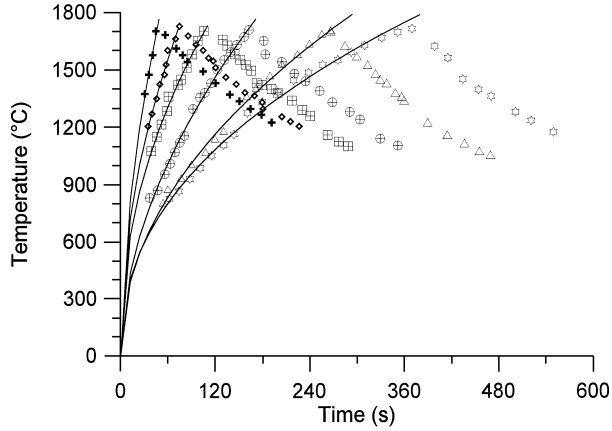

Fig. 7. Evolution of temperature of carbon crucible (within the H. F. furnace) according to different heating and cooling rates. Heating stages are fitted using the power law: $T = a.t^b$, with parameters as reported in Table 1.

Table 1. Calculated and experimental values derived from the study of grain growth during heating and cooling of the fibres[a]

a	b	c	$1400 < T < 1685°C$				$\Delta t_{exp}^{total}(s)$	G_{exp} (μm)	$1400 < T < 1700°C$	
			$\Delta t_{1685}^{heat}(s)$	t_{1685} (s)	Δt_{1685}^{total} (s)	G_{1685}^{calc} (μm)			Δt_{1700}^{total} (s)	G_{1700}^{calc} (μm)
—	—	1685	0	0	77·2	1·15			80·9	1·3
223·6	0·5579	1843	8·2	37·3	87·7	1·21	87	1·16	92·4	1·37
203·7	0·5337	1911	15·4	52·4	92·5	1·24			97·2	1·39
185·5	0·5115	2016	22·7	74·7	99·9	1·27	93		104·9	1·43
169·9	0·4924	2171	33·1	105·6	110·3	1·33	111		118·3	1·5
161·8	0·4825	2293	40·9	128·4	118·2		120	1·49		
158·2	0·4782	2362	45·2	140·7	122·4	1·37				
149·1	0·4671	2594	58·8	179·7	136·0	1·42	130	1·37		
140·0	0·4560	2955	78·2	234·1	155·4	1·49			143·2	1·60
130·9	0·4449	3562	106·3	311·9	183·4	1·58			193·3	1·79
121·9	0·4338	4675	147·8	425·2	225·0	1·7	215	1·75		
112·8	0·4227	7125	213·2	600·8	290·4	1·86			306·5	2·11

[a]a and b are the parameters used to fit experimental heating stages according to relation eqn (5): $T_{heat} = a \cdot t^b(^\circ C)$. c is the parameter used to fit experimental cooling schedule according to relation eqn (6): $T_{cool} = c \cdot \exp(-d \cdot t)(^\circ C)$ where $d = 0{\cdot}0024\ s^{-1}$. Δt_{1685}^{heat} represents the time needed to heat a sample from 1400 to 1685°C, t_{1685} the time needed to reach a 1685°C maximum temperature and Δt_{1685}^{total} the total processing time (heating and cooling stages) for temperatures between 1400 and 1685°C. $G_{1685}^{calc}$is the calculated average grain size obtained from relation eqn (11) and previous a, b and c values, assuming that the maximum temperature was $T_{max} = 1685^\circ C$. $\Delta t_{exp}^{total}(1400 < T < 1685^\circ C)$ and G_{exp} are experimental values. Δt_{1700}^{total} and G_{1700}^{calc} reported in the last columns are values calculated with a maximum temperature: $T_{max} = 1700^\circ C$.

all experiments ($d = 2{\cdot}4 \times 10^{-3}\ s^{-1}$). For example, the time needed to cool the sample from 1700 to 1400°C was about 81 s.

For some of these experiments, average grain size was measured and is reported in Fig. 8 versus 'processing time' at temperature above 1400°C. The 'processing time' parameter corresponds to the sum of the times needed first to heat the sample from 1400 to 1700°C and then to cool it from 1700 to 1400°C assuming no soaking time. It is related to heating and cooling rates through the above relations. In all cases, the average grain size is higher than 1·16 μm, and is equal to 1·75 μm for a 215 s heat treatment above 1400°C.

3.3.2 *Determination of the grain growth law of alumina fibres*

Classic models express the grain growth rate in ceramics as:[10]

$$\frac{dG}{dt} = \frac{K}{G^{m-1}} \tag{7}$$

where G is the grain size, m is an exponent related to the diffusion mechanism and K is a constant at a given temperature including characteristics of the studied material such as molar volume, surface energy, diffusion coefficient. For a given temperature, integration of relation eqn (7) gives rise to the well known equation:

$$G^m - G_o^m = K \times t \tag{8}$$

where G_o is the initial grain size. K can be detailed as:

$$K = k_o \cdot \frac{\gamma}{T} \cdot \exp\left(-\frac{Q}{RT}\right) \tag{9}$$

where k_o is another constant, γ is the specific grain boundary energy, T is the temperature, Q is the

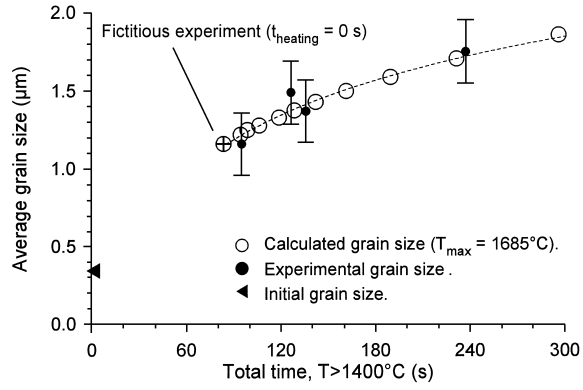

Fig. 8. Average grain size measured on samples heat treated according to processing schedules such as those given in Fig. 7. Total time includes heating and cooling times. Calculated grain sizes determined from relation eqn (11) with a maximum temperature of 1685°C are also reported. The ⊕ point corresponds to the fictitious end point experiment where the sample would be instantaneously heated at 1685°C (heating time = 0 s) and cooled in the furnace (cooling time = 77 s).

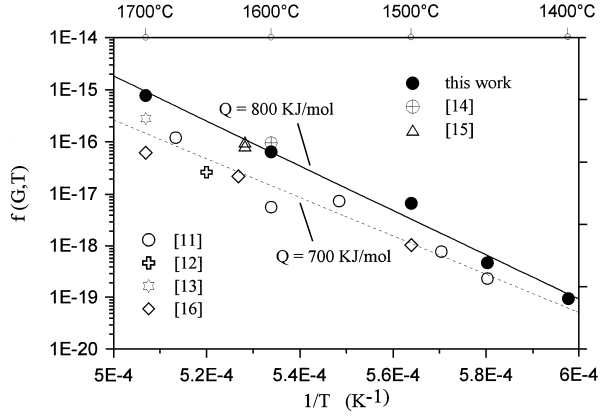

Fig. 9. Arhenius plot of grain growth evolution as a function of $1/T$ where $f(G, T) = [G^3 - G_o^3] \cdot T/\gamma \cdot t$ which corresponds to relation eqn (10):$[G^m - G_o^m] \cdot T/\gamma \cdot t = k_o \cdot \exp(-Q/RT)$. Results from other works[11–16] dealing with alumina grain growth are reported in the same manner.

activation energy corresponding to the predominant diffusion mechanism and R is the gas constant.[10] Rewriting relation eqn (8) with expression eqn (9) gives:

$$\frac{[G^m - G_o^m]\cdot T}{\gamma\cdot t} = k_o\cdot\exp(-Q/RT) \qquad (10)$$

Provided k_o remains constant over the studied range, the representation of experimental points $(G(t, T))$ in an Arrhenius plot must give a straight line for the (m, Q) couple, characteristic of the preponderant diffusion mechanism controlling grain growth. In order to determine values of m and Q for the studied fibres, the alumina boundary energy was taken from the Nikopoulos relation for γ_{SS}[6] and the initial grain size measured as $G_o = 0.3\ \mu$m. A least square fit analysis on relation eqn (10), using isothermal grain size measurements performed at different temperatures, allowed us to deduce the corresponding mechanism and activation energy. Figure 9 shows the Arrhenius representation with $m = 3$ which gives the best alignment of our data. This cubic grain growth kinetics is in good agreement with other works dealing with alumina[11–16] and is attributed to impurity drag limited grain growth[10]. Values calculated from Bennison[14] and Zhao[15] who measured grain size on dense samples, lie well on our fit which gives an activation energy $Q \approx 800$ kJ mol^{-1}. A slight difference can be observed with the value of the energy obtained from other data which could easily be attributed to differences in MgO impurity levels existing between these alumina samples.

3.3.3 Modelling of grain growth as a function of the heating and cooling kinetics

As previously mentioned, grain growth within fibres really started for annealing temperatures higher than 1300°C (Fig. 3). Therefore, the study was focused on the 1400–1700°C temperature range. Knowing the value of the activation energy, Q, grain growth evolution can be calculated from integration of relation eqn (7) where temperature is related to time through the mathematical functions eqn (5) and eqn (6), describing heating and cooling steps. k_o is assumed to remain constant over the considered temperature range and is deduced from the y intercept at $1/T = 0$ on Fig. 9 ($k_o = 1.2 \times 10^6$ m^3 K s^{-1}). The expression of surface energy is taken from Nikopoulos[6]. Then, G can be written as a function of t:

$$G^3 - G_o^3 = \int_{t_{1400°C}}^{t_{T\max}} \frac{k_o\cdot\gamma}{a\cdot t^b + 273}\cdot\exp\left(\frac{Q/R}{a\cdot t^b + 273}\right)\cdot dt + \int_{t_{T\max}}^{t_{1400°C}} \frac{k_o\cdot\gamma}{c\cdot e^{-dt} + 273}\cdot\exp\left(\frac{Q/R}{c\cdot e^{-dt} + 273}\right)\cdot dt \qquad (11)$$

In fact, the only adjustable parameter remaining in relation eqn (11) is the maximum temperature reached during the experiment, T_{max}. Different T_{max} values, close to 1700°C, were tested to calculate grain sizes; these sizes were then compared to the experimental ones obtained when the maximum temperature of the furnace was aimed to be 1700°C. Figure 8 reports these calculated values with $T_{max} = 1685$°C, versus total time ($T >$ 1400°C), i.e. for different heating kinetics. A rather good agreement is observed between experimental and calculated grain size. The result of this calculation appears significant and consistent: first, the real temperature of fibres cannot be higher than that of the crucible (aimed to be 1700°C) and second, a 15°C temperature difference seems quite reasonable considering the used heating device.

It is now possible to determine the best parameters of the preparation process that would limit grain growth within the alumina fibre and therefore that will allow this reinforcement to play its role in the mechanical properties of the composite.

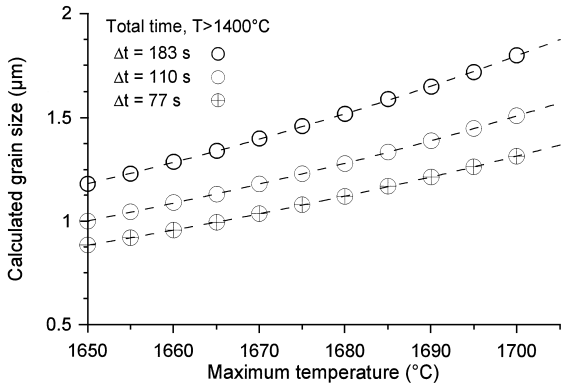

Fig. 10. Influence of the maximum temperature on calculated grain size for different heating and cooling rates.

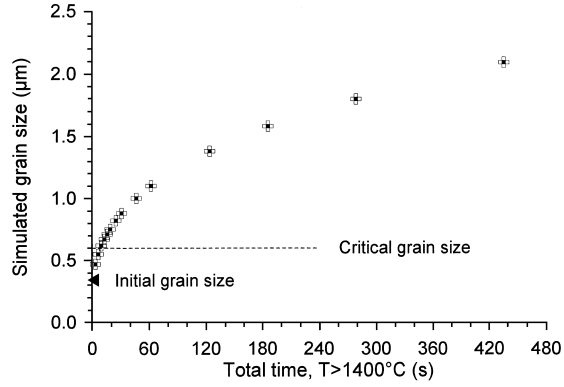

Fig. 11. Calculation of grain size assuming that the maximum temperature is 1685°C and that times needed to heat and cool the samples from 1400 to 1685°C are identical.

According to manufacturer's data, a large decrease of the fibre failure strength is observed when the grain size is higher than $0{\cdot}6\,\mu$m. Nevertheless, Fig. 8 shows that, for a 1685°C heat treatment, the grain size will always be higher than one micron using the experimental device as designed. According to our calculation, the smallest grain size that is possible to obtain is $1{\cdot}16\,\mu$m (point $\oplus$) and even this corresponds to a fictitious experiment where the infiltration of the liquid alloy would be instantaneous ($t_{\text{heating}} = 0$ s), the cooling stage ($t_{\text{cooling}} = 77$ s) only being responsible for grain growth. Influence of $T_{\max}$ on final grain size was also investigated considering different processing kinetics. A $\sim 50\%$ variation in size is observed over a 50°C temperature range and, as expected, grain size evolution is larger for slower heating and cooling rates (Fig. 10). But, even at 1650°C for the shortest heat treatment, the grain size remains higher than $0{\cdot}8\,\mu$m. Therefore, the only way to control this liquid infiltration process relies on a large increase of the cooling rate. A simulation was carried out assuming identical heating and cooling times and a maximum temperature of 1685°C. Heating rate was still described by a power law such as relation eqn (5), while the cooling stage followed an exponential law such as relation eqn (6). Very short thermal heat treatments were considered and the results are presented in Fig. 11. The $0{\cdot}6\,\mu$m critical grain size is reached as soon as the total processing time (when $T > 1400$°C) exceeds 10 s. Such a short heating step is feasible using high frequency apparatus. On the other hand, the cooling step requires a quenching operation more than the usual cooling stage, a change which is certainly much more complicated to deal with due to the working atmosphere.

4 Conclusion

Grain growth phenomena within alumina fibres during high temperature processing of a NiAl/Al_2O_3 composite were studied. Experiments conducted as a function of the temperature for 1 h, showed that the grain size reached the diameter of the fibre between 1600 and 1700°C. Further heating led to a so-called 'bamboo configuration' and then to grain boundary grooving. Thermodynamic calculations, taking into account the presence of the liquid alloy, predicted a deepened grain boundary groove which was experimentally observed.

The kinetic modelling of grain growth during the heating and cooling steps was also investigated. A cubic grain growth law was observed and the activation energy of the process was estimated to be $800\,\text{kJ mol}^{-1}$. Calculation of grain sizes as a function of heating and cooling rates was performed and successfully compared to experimental values.

Such a modelling allowed us to study and determine the conditions of preparation of the NiAl/Al_2O_3 composite according to the liquid infiltration method which implies high temperature treatments and consequently growth of the grains in the fibres. For applications, grain sizes within the alumina fibres should remain less than $\sim 0{\cdot}6\,\mu$m to avoid drastic degradation of the mechanical properties.[2,9] Our modelling shows, first, that at 1685°C this condition cannot be fulfilled even for an instantaneous heating step. Second, even a decrease of the maximum temperature down to 1650°C is not sufficient to limit grain growth to an acceptable value, due to the length of the cooling stage. Therefore, the only way to process the material is to consider much more rapid processing treatments above 1400°C (< 10 s) which almost require a quenching of the material for the cooling step.

References

1. Dariola, R., Lahrmann, D. F. and Field, R. D., In *Ordered Intermetallics, Physical Metallurgy and Mechanical Behavior*, eds. C. T. Liu, R. W. Cahn and G. Sauthoff. Kluwer Academic, Dordrecht, 1992, pp. 679–698.
2. Bihr, J. C., The NiAl/Al_2O_3 composite material. Ph.D. thesis, University of Bordeaux, France, 1996.
3. Silvain, J. F., Bihr, J. C., Alnot, M., Lambert, J. and Ehrhardt, J. J., X-ray photoelectron spectroscopy and transmission electron microscopy studies of the NiAl/Al_2O_3 interfacial chemical compatibility. *J. Vac. Sci. Technol.*, 1995, **A13**, 1983–1900.
4. Miller, K. T. and Lange, F. F., The morphological stability of polycristalline fibers. *Acta. Metall.*, 1989, **37**, 1343–1347.
5. Fullman, R. L., Measurement of particle sizes in opaque bodies. *Trans. AIME*, 1953, **197**, 447–452.
6. Nikopoulos, P., Surface, grain boundary and interfacial energies in Al_2O_3 and Al_2O_3–Sn, Al_2O_3–Co systems. *J. Mater. Sci.*, 1985, **20**, 3993–4000.
7. Ayushina, G. D., Levin, E. S. and Gel'd, P. V., Effect of temperature and composition on the density and surface energy of molten alloys of aluminum with cobalt and nickel. *Zh. Fiz. Khim. Russ.*, 1969, **43**, 2756–2760.
8. Lavaste, V., Mechanical behaviour and morphological evolution of alumina based ceramic fibres. Ph.D. thesis, E.N.S Mines of Paris, 1993.
9. Kovar, D. and Ready, M. J., Role of grain size in strength variability in alumina. *J. Am. Ceram. Soc.*, 1994, **77**, 1928–1938.
10. Brook, R. J., Controlled grain growth. In *Treatise on Material Science and Technology*, ed. F. F. Wang. Vol. 9. Academic Press, New York, 1976, pp. 331–362.
11. Coble, R. L., Sintering cristalline solids. II, Experimental test of diffusion models in powder compacts. *J. Appl. Phys.*, 1961, **32**, 793–799.
12. Jorgensen, P. J. and Westbrook, J. H., Role of solute segregation at grain boundaries during final stage sintering of alumina. *J. Am. Ceram. Soc.*, 1964, **47**, 332–338.
13. Mocellin, A. and Kingery, W. D., Microstructural changes during heat treatment of sintered Al_2O_3. *J. Am. Ceram. Soc.*, 1973, **56**, 309–314.
14. Benison, S. and Harmer, M. P., Grain growth kinetics for alumina in the absence of a liquid phase. *J. Am. Ceram. Soc.*, 1985, **68**, C22–24.

15. Zhao, J. and Harmer, M. P., Sintering of ultra high purity alumina doped simultaneously with MgO and FeO. *J. Am. Ceram. Soc.*, 1987, **70**, 860–866.

16. Janney, M. A., Kimrey, H. D., Schmidt, M. A. and Kiggans, J. O., Grain growth in microwave-annealed alumina. *J. Am. Ceram. Soc.*, 1991, **74**, 1675–1681.